Journal of Advanced Electrochemistry 1(1) (2015) 19–24

ISSN: 2455-0205

Contents List available at JACS Directory

Journal of Advanced Electrochemistry

journal homepage: http://www.jacsdirectory.com/jaec

Electrochemical Study of Some Schiff Base by Cyclic Voltammetry and Its Metal Complex - DNA Interaction Study by UV-Visible Spectroscopy

R. Das*, A. Saxena, S. Saxena, G. Khan

Department of Chemistry, Dr. Hari Singh Gour Central University, Sagar – 470 003, MP, India.

ARTICLE DETAILS

Article history:
Received 22 September 2015
Accepted 13 October 2015
Available online 03 November 2015

Keywords:
Schiff Base
Carbon Paste Electrode
Cyclic Voltamtery
DNA interaction
UV-Visible Spectroscopy

ABSTRACT

Present paper investigate the electrochemical behaviour of isatin-3-hydrazone derivative i.e. A, B, C mentioned in manuscript and its interaction with salmon sperm fish DNA. Electrochemical study of these compounds done in 0.02 M phosphate buffer and 0.1 M LiCl used as a supporting electrolyte at carbon pest electrode by cyclic voltamtery (CV). CV study reveal that all synthesized compound show $2e^-$ diffusion control, irreversible reduction peak and the product of this reduction are secondary amines. The diffusion coefficients of these derivatives were also calculated. After that DNA-interaction study of its metal (Cd) complex done by UV-Visible spectrophotometer that show metal cation (Cd^{+2}) or protonated nitrogen atom of these metal complexes probably interact with O atom of phosphate group in DNA back bone by electrostatic attraction force and the result of these type of interaction are denaturation of DNA strand which seem by hyperchromism in the emission spectra of these complex. Binding/association constants of these complexes were also calculated in this paper.

1. Introduction

The indole is strong pharmacodynamic moiety and possesses important biological properties such as anti-inflammatory, antibacterial, anticonvulsant, antioxidant properties [1-3]. Isatin i.e. indole 2,3 dione is also synthetically versatile heterocyclic compound is known to act as a potent endogenous neurochemical regulator in brain of mammals [4,5] and isatin also work as modulator of different kind of biochemical processes like inhibitor of monoamine oxidase(MAO) and later on identified as a selective inhibitor of monoamine oxidase B [6,7]. Further investigation has proved that isatin work as an antagonistic of both atrial natriuretic peptide stimulated [8] and nitric oxide stimulated [9] guanylate cyclase activity.

On other hand rout for the synthesis and metabolism of isatin and its derivatives in animal tissues have not been fully recognized. It has been assumed that isatin is formed in the tissues from phenylalanine or tryptophan [10, 11]. *In vitro* isatin can be destroyed easily by high concentration of hydrogen peroxide. In addition to isatin is easily metabolized by xanthine oxidase, producing hydrogen peroxide by the formation of superoxide [10, 12]. However, at this level it is not clear whether this mechanism operate also *in vivo.*

Further study has shown that isatin and its derivatives possess broad range of application in synthetic, biological, and clinical activity. It has shown oxidation and reduction at glassy carbon electrode. The oxidation of isatin was found to be pH dependent and the reduction of isatin was irreversible and show two consecutive electron transfer reaction, this study done by CV [13].

The electrochemical determination of isatin [14] and other nitrogen containing heterocycles taking variety of electrode systems [15, 16] attain a distinguished position in recent years. 3-arylimino derivatives (Schiff bases) obtained by the condensation of aromatic amines with isatin, are powerful antibacterial, anticonvulsant, antiviral and anti-fungal agent [17-19]. Copper (π) complex with isatin Schiff base ligand are potential antitumor agent [20]. Recent achievement indicate isatin interact with wide range of monoamine in the biological systems [21]. Investigation of electrochemical behavior of biologically important compound by electrochemical technique like cyclic voltamtery, DPV, SWV have efficiency for giving valuable information like redox properties of biologically important compound, its reduction or oxidation potential and stability in the body fluid etc. For this purpose today, voltammetric technique have been successfully used due to its high sensitivity [22-25].

DNA is the pharmacological target of many of the drugs that are currently in clinical use or in advanced clinical trials. DNA that is target molecule regulate the cell function by work on translation and transcription, small molecule that may be ligand or complex molecule bind to DNA and alter the cell function by changing these two process i.e. translation or transcription, these ligand molecule or complex molecule work as a drug, and show inhibition or alteration of DNA function by changing its structure so this is basic requirement to cure or control a particular disease [26].

For understanding the disease controlling or killing process, firstly we could know the mechanism of drug-DNA dealing. This is not only necessary for controlling the disease but also for designing a new drug. However the process of action between drug and DNA is still relatively little known. For performing these action *in vitro*, it necessary to produce more simple method for investigating the mechanism of action, and by understanding the mechanism we can design a new 'DNA' targeted drug [27]. Present study is concerned to give the information of redox behavior of some Schiff base by CV at carbon pest electrode and its interaction with deoxyribonucleic acid (DNA).

2. Experimental Methods

2.1 Chemicals and Apparatus

Chemicals purchased from Sigma-Aldrich, Himedia and used without purification. Melting point was determined by using open capillary tube melting point apparatus. The IR spectra were recorded on a FTIR Shimadzu-8400S spectrometer using KBr pellets. The 1HNMRand 13CNMR spectra were recorded on Varian 300 spectrometer taking TMS as standard and DMSO as a solvent. Sonication was done with the help of frontline sonicator (with a frequency of 22 KHz with a normal power of 225W). The P^H measurement was carried out by μ P^H system 361 digital pH meter.

2.2 Electrochemical Cells and Voltammetric Parameters

Voltammetric experiments were carried out using a Metrohm 797 V.A. Computrace (Swiss made). Cyclic voltammetry were carried out using a

*Corresponding Author
Email Address: ratneshdas1@gmail.com (R. Das)

Cite this Article as: R. Das, A. Saxena, S. Saxena, G. Khan, Electrochemical study of some Schiff base by cyclic voltammetry and its metal complex - DNA interaction study by UV-visible spectroscopy, J. Adv. Electrochem. 1(1) (2015) 19-24.

carbon paste electrode (d = 0.2 cm) as working electrode, a Pt wire as a counter electrode, and a Ag/AgCl (3 M KCl) as a reference electrode, in one-compartment electrochemical cell. Carbon paste electrode (d = 0.2 mm) were prepared by mixing graphite powder with paraffin wax in 3:7 ratio, then it was sonicated for 1 min in an ultrasound bath and again rinsed with water. After this mechanical treatment, the carbon pest electrode was placed in three cell system. This procedure ensured very reproducible experimental systronics 2201 double beam UV-Visible spectrophotometer were used for performing drug-DNA interaction. Emission spectra of complex were recorded on R-F-5301 flurometer.

2.3 Sample Preparation

For cyclic voltammetry (CV) solutions were prepared by mixing 7.0 mL of 0.01M stock solution and 1.0 mL of 0.1 M LiCl (as supporting electrolyte) and 2.0 mL of 0.2M appropriate (phosphate) buffer. Nitrogen gas was passed in the solution for ~15 minutes and, thereafter, a blanket of nitrogen gas was maintained throughout the experiment. During the experiment solution was subjected to controlled potential electrolysis. For UV-Visible study Salmon fish sperm DNA was used without further purification, its concentration was identified spectrophotometrically using the molar absorption coefficient ε_{277}=2480 $cm^{-1}mol^{-1}$. But here known concentration are used that are 0.001, 0.0016, 0.00232, 0.00476 M and its 1.1, 1.6, 2.32, 4.76 mL volume will taking for analysis.

2.4 Synthesis of Isatin-3-Hydrazone Derivatives

Isatin-3-hydrazone and appropriate aldehydes and ketones were dissolved in 30 mL DMF in presence of protonation reagent (Scheme 1) i.e. glacial acetic acid (0.01 mL) was kept at 60 °C on water bath for 30 min with continuing stirring. The purity of compounds was checked by TLC using Merck pre-coated gel GF aluminum plates. Benzene: chloroform: methanol taking as a mobile phase. The reaction mixture was poured into water (300 mL) and recrystallization done by ethanol as a solvent.

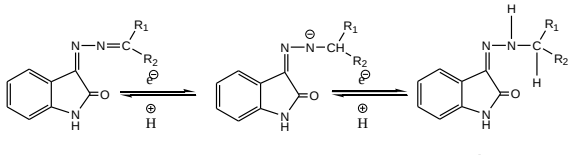

compound	R_1	R_2
2a	CH_3	C_2H_5
2b	C_6H_4Cl	H
2c	C_6H_5	CHO

Scheme 1 Synthesis of isatin-3-hydrazone derivative

2.4.1 Isatin -3-(methyl ethylide)-hydrazone ***(2a)*****:** FTIR (KBr) (V_{max} cm^{-1}): 3470 (N-H), 1670 (C=O), 1590 (C=C), 1220 (C-O), 3315 (N-N) 1346 (C-N), 787 (C-Cl). ^{1}HNMR (300 MHz, DMSO, TMS, δppm): 7 (m, 8H, H_{Ar}), 9.5 (d, 1H, NH), 3.3 (s, 3H, CH_3), 10.7 (s, 1H, H_{enolic}); ^{13}CNMR (400 MHz, $CDCl_3$, δppm) δ_c: 40, 110, 125, 165.

2.4.2 Isatin-3-(2-chlorobenzylidene)-hydrazone ***(2b)*****:** FTIR (KBr) (V_{max} cm^{-1}): 3470 (N-H), 1670 (C=O), 1590 (C=C), 1220 (C-O), 3315 (N-N) 1346 (C-N), 787 (C-Cl). ^{1}HNMR (300 MHz, DMSO, TMS, δppm): 6.7 (m, 8H, H_{Ar}), 7.3 (s, 1H, NH), 2.5 (S, 1H, CH); ^{13}CNMR (400 MHz, $CDCl_3$, δppm) δ_c: 170, 75, 110.

2.4.3 Isatin-3-(benzylidene)-hydrazone ***(2c)*****:** FTIR (KBr) (V_{max} cm^{-1}): 2980 (CH), 1690 (C=O), 1610 (C=C), 1270 (C-O), 1180 (C-N). ^{1}HNMR (400 MHz, $CDCl_3$, TMS, δppm): 3.38 (s, 1H, =CH), 7.5 (m, 9H, H_{Ar}), 9.5 (d, 1H, NH), 10.7 (s, 1H, H_{enolic}), 2.19 (t, 3H, CH_3),; ^{13}CNMR (300 MHz, DMSO, δppm) δ_c: 165, 126, 110, 40.

3. Results and Discussion

3.1 Cyclic Voltammetric Studies

This paper explains the electrochemical behaviour of Isatin-3-hydrazone derivatives at a carbon paste electrode and this experiment were carried out in 0.2 M phosphate buffer and 0.1 M LiCl as supporting electrolyte. Compound 2a and 2c, 2b (each has 0.01 M concentration) show voltammograms at 10 pH and 5 pH respectively. During the voltammetric measurement a constant flux of N_2 was kept over the solution surface in order to check the diffusion of atmospheric oxygen into the solution. In this study purging time is 10 s, deposition time is 60 s. and deposition potential is -0.9 V. Several peaks were observed (Fig. 2, 5, 7, 9). A study of effect of scan rate is made in order to find out the mechanism and the feasibility of electrochemical reactions and linear plots of I_{pc} *vs* $V^{1/2}$ are obtained, that show the reduction of derivatives in this medium is diffusion controlled with increasing scan rate (Fig. 1).

3.2 Isatin-3-Hydrazone

Isatin-3-hydrazone shows one electron reduction peak on different scan rate. It's anodic half cycle and cathodic half cycle show one peak as mentioned in table1 and shown in Fig. 2. Good linear plots of I_{pc} *vs* $v^{1/2}$ are obtained that show the reduction of isatin-3-hydrazone in this medium is diffusion controlled with employed scan rate (30 to 50 mVs^{-1}) in Fig. 4. The shift of cathodic peak potential towards more positive values with the increase in scan rate indicates irreversible nature of the system [28].

The peak potential of irreversible reaction is given by the following equation

$$E_p = E^0 - (RT/\alpha n_a F)[0{\cdot}78 - \ln(k^0/D^{1/2}) + \ln(\alpha n_a Fv/RT)^{1/2}] \quad (1)$$

Where α is the cathodic charge transfer coefficient, n_a is the number of electrons involved in the charge transfer step, D_0 the diffusion coefficient. Peak current for irreversible system is given by Randle Sevick equation

$$I_{pc} = (2{\cdot}99 \times 10^5)\, n\, (\alpha n_a)^{1/2}\, A C D_0^{\,1/2} v^{1/2} \quad (2)$$

Where A is the area of electrode in cm^2, D_0 the diffusion coefficient in cm^2 s^{-1}, C the concentration in $molL^{-1}$ and ν is in mVs^{-1}.

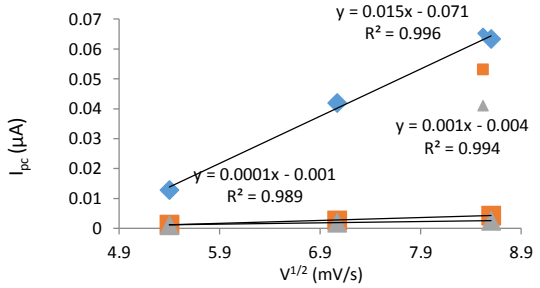

Fig. 1 Plot of peak current (I_{pc}) *vs* square root of the sweep rate ($v^{1/2}$) for 2a(blue), 2b(red), 2c(green)

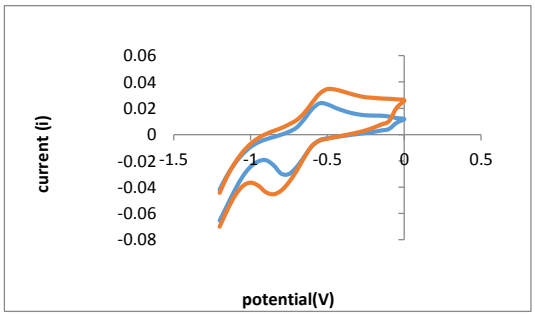

Fig. 2 Cyclic voltammogram of isatin-3-hydrazones at different scan rates

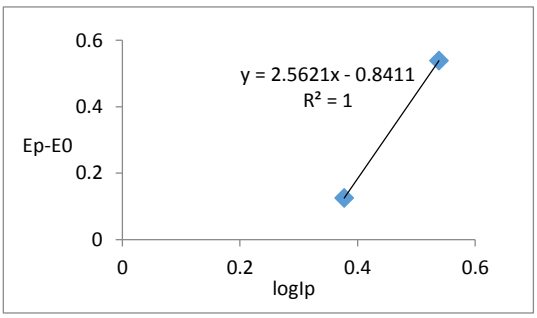

Fig. 3 Plot of Ep-E_0 *vs* logIp for isatin-3-hydrazone

Plot In(Ip) vs $E_p - E^0$ determined at different scan rates has a slope of equal to $-0{\cdot}542/\alpha n_a$ so by the use of this slope value we can find the charge transfer coefficient α in Fig 3 and D_0 values for isatin-3-hydrazone can be determined from the slope of plot I_{pc} vs $v^{1/2}$ (Fig. 4). In this calculation (Fig. 3) slope equal to 2.562 and intercept equal to -0.841, charge transfer coefficient α equal to 0.211.

Cite this Article as: R. Das, A. Saxena, S. Saxena, G. Khan, Electrochemical study of some Schiff base by cyclic voltammetry and its metal complex - DNA interaction study by UV-visible spectroscopy, J. Adv. Electrochem. 1(1) (2015) 19-24.

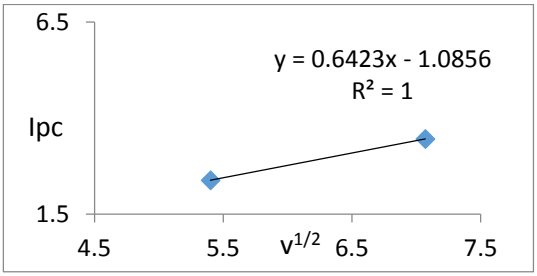

Fig. 4 Plot of peak current (Ipc) vs square root of the sweep rate ($v^{1/2}$) for isatin-3-hydrazone

Table 1 Electrochemical parameters of isatin-3-hydrazone

Ep_c (mV)	Ip_c (pA)	Scan rate (mVs^{-1})	Ep_a (mV)	Ip_a (pA)	$D_0^{1/2}x10^{-3}$ (cm^2s^{-1})
-0.54932	2.383	30	-0.79956	-2.9735	0.107
-0.49927	3.4557	50	-0.84961	-4.5452	0.119

3.3 Compound 2a

Compound 2a shows two peaks each have one electron reduction behaviour. Anodic half cycle show two peak but cathodic half cycle does not show any peak in Table 2, Fig. 5. Linear plots of I_{pc} vs $V^{1/2}$ are obtained that show reduction of Schiff base is diffusion controlled within varied scan rate in Fig. 1. The shift of Cathodic peak potential towards more positive values with the increase in scan rate indicates irreversible nature of the system.

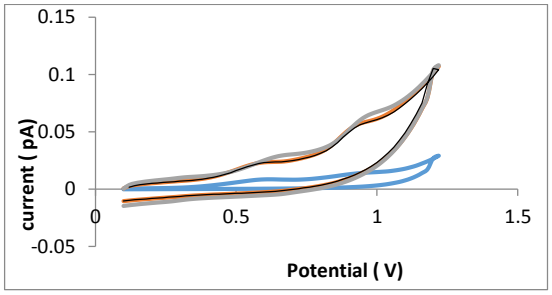

Fig. 5 Cyclic Voltammogram of (2a) isatin-3[methyl ethylidene] hydrazones at different scan rate

Table 2 Electrochemical parameters of Isatin-3-[methyl ethylidene] hydrazones (Here we take only 1 peak for calculation)

Scan rate (mVs^{-1})	Ep_c (mV)	Ip_c (pA)	$D_0^{1/2}x10^{-6}$ (cm^2s^{-1})
30	0.87952	0.01292	1.2
50	0.91949	0.055966	3
75	0.95947	0.063378	3.7

Plot In(Ip) vs $E_p - E^0$ determined at different scan rates has a slope of equal to $-0{\cdot}542/\alpha n_a$ so by the use of this slope value we can find the charge transfer coefficient α in Fig. 6 and D_0 values for Schiff bases 2a can be determined from the slope of plot I_{pc} vs $v^{1/2}$ Fig. 1. In this calculation (Fig. 6) slope equal to 0.537 and intercept equal to 0.539, charge transfer coefficient α equal to 0.50.

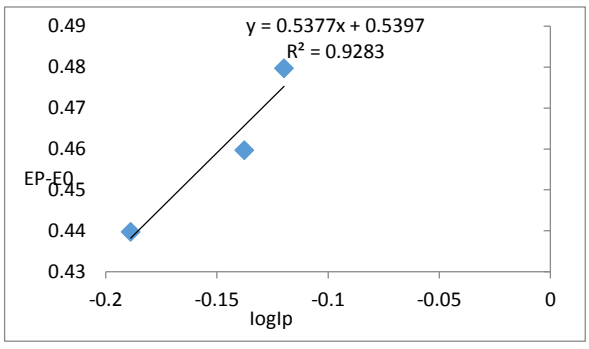

Fig. 6 Plot of log Ip *vs* E_P-E_0 for compound 2a

3.4 Compound 2b

Schiff bases 2b show one electron reduction peak for scan rate 30 to 75 mVs^{-1}. Anodic and cathodic half cycle show one peak Fig. 7. Good linear plots of I_{pc} vs $v^{1/2}$ are obtained. That shown the reduction of Schiff base in this medium is diffusion controlled Fig. 1. Variation in peak position as a function of scan rate means irreversible nature of the system (Fig. 7).

Table 3 Electrochemical parameters of isatin-3-[2 chloro benzylidene] hydrazones.

Scan rate (mVs^{-1})	Ep_c (mV)	Ip_c (pA)	$D_0^{1/2}x10^{-6}$ (cm^2s^{-1})
30	-0.50049	0.0012697	2.0
50	-0.44052	0.0026876	4.0
75	-0.3006	0.0043569	5.0

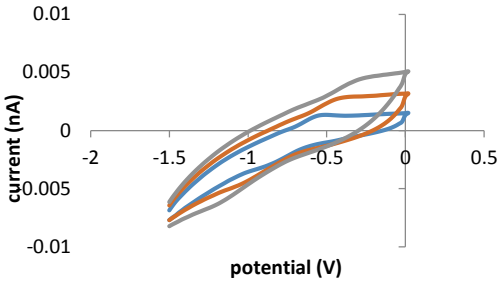

Fig. 7 Cyclic Voltammogram of isatin-3-[2-chlorobenzylidene]hydrazones at different scan rate

Plot In(Ip) vs $E_p - E^0$ determined at different scan rates has a slope of equal to $-0{\cdot}542/\alpha n_a$ so by the use of this slope value we can find the charge transfer coefficient α in Fig. 8 and D_0 values for Schiff bases 2b can be determined from the slope of plot I_{pc} vs $v^{1/2}$ Fig. 1. In this calculation (Fig. 8) slope equal to 2.063 and intercept equal to -3.280, charge transfer coefficient α equal to 0.26.

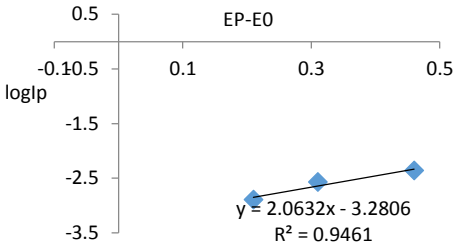

Fig. 8 Plot of log Ip *vs* E_P-E_0 for compound 2b at 0.01 M concentration

3.5 Compound 2c

Schiff bases 2c show one electron reduction peak for scan rate 30 to 75 mVs^{-1}. Cathodic half cycle show one peak (Fig. 9). Good linear plots of I_{pc} vs $v^{1/2}$ are obtained that show the reduction of Schiff base in this medium is diffusion controlled Fig1. Variation of peak position as a function of scan rate means irreversible nature of the system.

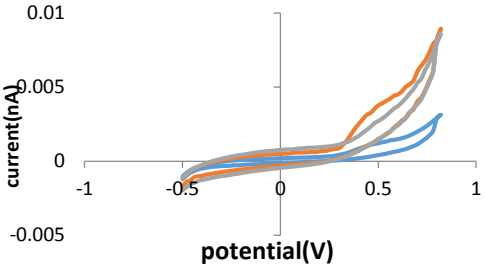

Fig. 9 Cyclic voltammetry of isatin-3-[benzylidene] hydrazone at different scan rate

Table 4 Electrochemical parameters of Schiff bases, isatin-3-[benzylidene] hydrazones

Scan rate (mVs^{-1})	Ep_c (mV)	Ip_c (pA)	$D_0^{1/2}x10^{-7}$ (cm^2s^{-1})
30	0.45959	0.0011458	2.1
50	0.47958	0.002003	3.1
75	0.49957	0.00255	5.3

Cite this Article as: R. Das, A. Saxena, S. Saxena, G. Khan, Electrochemical study of some Schiff base by cyclic voltammetry and its metal complex - DNA interaction study by UV-visible spectroscopy, J. Adv. Electrochem. 1(1) (2015) 19-24.

Plot In(Ip) vs E_p–E^0 determined at different scan rates has a slope of equal to $-0{\cdot}542/\alpha\ n_a$ so by the use of this slope value we can find the charge transfer coefficient α in Fig 10 and D_0 values for Schiff bases 2b can be determined from the slope of plot I_{pc} vs $v^{1/2}$ (Fig. 1). In this calculation slope equal to 1.595 and intercept equal to -3.227, charge transfer coefficient α equal to 0.34.

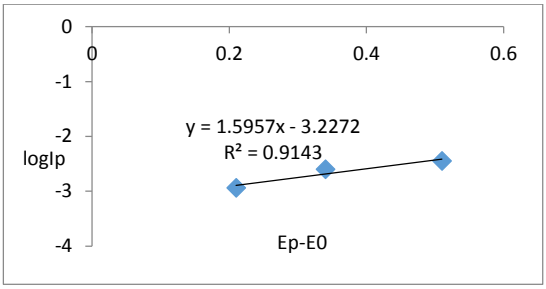

Fig. 10 Plot of log Ip *vs* E_P-E_0 for Compound 2c 0.01M at concentration

3.6 Effect of Concentration

With decreasing concentration of compound 2a, 2b, 2c from 0.01 M, 0.005 M, 0.0025 M peak current decrease but peak potential remains unaffected.

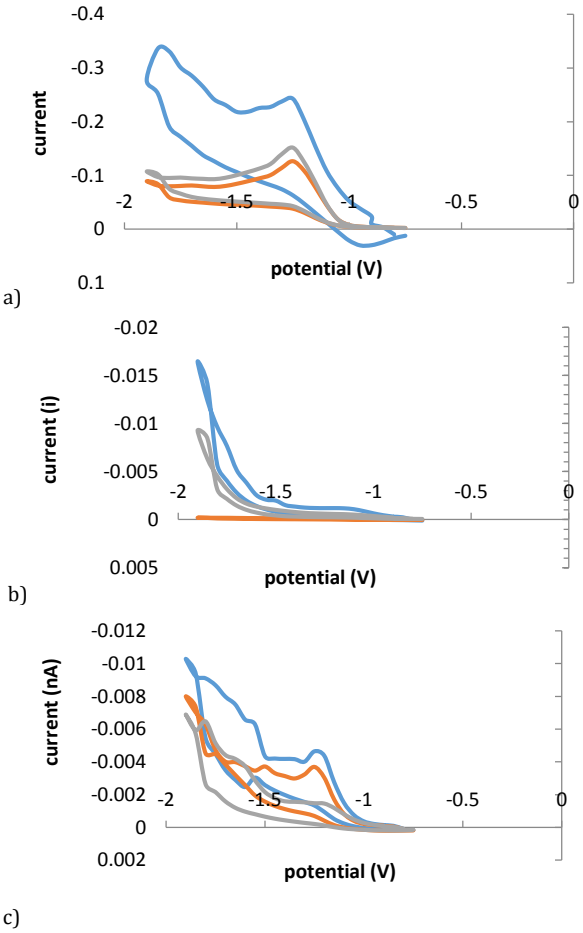

Fig. 11 Effect of concentration on peak current for compound (2a-2c)

4. Metal complex –DNA Interaction Study BY UV-Visible Spectroscopy

UV–visible absorption spectroscopy is very useful technique for study the drug alone or interaction with others molecules they may be small or large. It is very simplest, reliable and most commonly employed technique for study the drug–polynucleotide interaction. Drug-polynucleotide interaction are based on the absorption phenomena in the UV spectroscopy means each molecule show maximum absorption at particular wavelength, when these molecule interact with other molecule which may be small or large show maximum absorption at different wave length so, by analyzing the changes in the absorption properties (including λ_{max} or intensity of band) of drug and the drug-DNA complex, we can find the type of interaction between them. Generally drug works as a ligand exhibit an absorption maxima that can easily recognize in the visible region. an easy route for the determining the interaction between Drug and polynucleotide (or protein or enzyme) is to scan the shifting the position of the absorption maximum when drug is free in the solution or when the drug is attached with polynucleotide. The magnitude of this displacing of the absorption band could explain as a signal for the analyzing the strength of the interaction between the DNA and drug molecule [29-32].

Drug-polynucleotide (DNA) interaction are different type it could covalent or non-covalent depends upon the force that present between them ,which are identify by comparing the UV spectra of drug molecule and drug-DNA complex. If after interaction spectra show hypochromism and bathochromic shift (red shift) then its mean compound attached with DNA through intercalation. Degree of hypochromism is depends on the strength of intercalation [33], and strength of intercalation depends on the distance between DNA and drug molecule, when distance decrease then intensity of absorption band decrease result an hypochromic shift and in this case difference between π bonding and π* energy level also decrease, so electron transition from π bonding orbital of drug to π* orbital of polynucleotide easily takes place then result a red or bathochromic shift [34, 35].

On other hand hyperchromic effect is observed when drug molecule attach with DNA by electrostatic attraction (presence of cation), hyperchromism also reflect the structural or conformational changes in DNA molecule after binding with drug molecule, this phenomena occur due to presence of charged cation in the drug molecule, charge cation bind with more electro negative oxygen atom of phosphate group present on DNA back bone by electrostatic attraction [36] then hydrogen bonding between purine and pyrimidine base disrupted (A and T, G and C) and DNA denaturation takes place, by DNA denaturation purine and pyrimidine base are free as a result surface area (active site) increase so, the absorption intensity of band extremely increase about 40% more than free double strand DNA at the same concentration.

In the second part of this paper comprise the reaction of metal (Pb ,Cd) with compound 2a, 2b, 2c and by analyzing the fluorescence emission spectra e of these metal complex, result show that , these compounds formed complex with Cd more efficiently then Pd and after the formation of these metal complex the next step is to find out the interaction of these complex with polynucleotide molecule (DNA) because in the metal complex there have two possibility for binding of these complex with DNA molecule, first is to bind with DNA through metal cation and second is to bind with DNA by easily protonated nitrogen atom because fused polyaromatic system containing protonated nitrogen atom are typically work as intercalators.

On the bases of maximum absorption in free drug and drug combine with DNA we can find out the binding /association constant of the drug with DNA according to benesi-hildebrand equation [37].

$$A_0/A\text{-}A_0 = \varepsilon_D/\varepsilon_{D\text{-}D}\text{-}\varepsilon_D + \varepsilon_D/\varepsilon_{D\text{-}D}\text{-}\varepsilon_D \times 1/K_b\,[DNA] \qquad (3)$$

Where K_b is the association/binding constant,A_0, and A are the absorbance of drug and its complex with DNA, respectively, and $\varepsilon_{D\ and}$ $\varepsilon_{D\text{-}D}$ are the absorption coefficient of the drug and the DNA-drug complex, respectively. The association constant can be determined from the intercept-to-slope ratios of$A_0/A\text{-}A_0$ *vs.* 1/[DNA] plot.

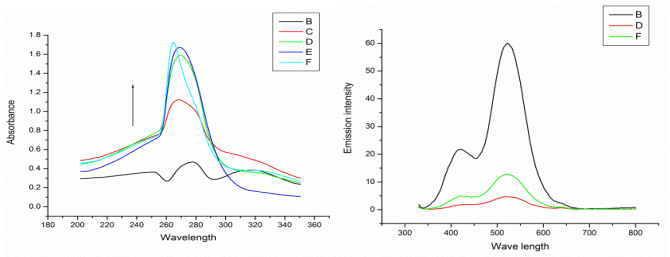

Fig. 12 (a) UV visible absorption spectra of $C_{12}H_{13}N_3O$ Cd Cl_2-DNA Complex and arrow represent the increasing concentration of DNA in the solution. (b) Emission of metal ($CdCl_2$) and ligand

Fig. 12 (a) show the interaction of $C_{12}H_{13}N_3O$ $CdCl_2$ complex with DNA, this show with increasing concentration of DNA in the drug solution the intensity of absorption band increase and λ_{max} also affected, so the consequence of DNA addition is hyperchromism and slight blue shift appear.

Fig. 13 represents the plot between A0/A-A0 *vs.* 1/[DNA], with the help of this plot we can determine the binding constant of Drug-DNA complex i.e. K_b = 3.8

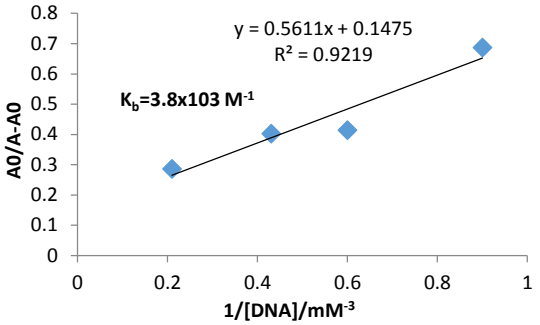

Fig. 13 Graph between A0/A-A0 *vs.* 1/ [DNA] plot

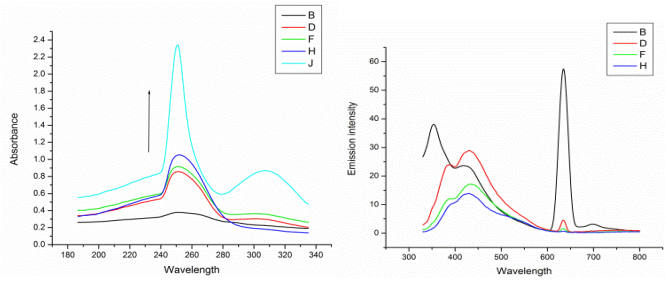

Fig. 14 (c) UV visible absorption spectra of $C_{15}H_{10}N_3ClO$ $CdCl_2$-DNA complex and arrow represent the increasing concentration of DNA in the solution. (D) Emission spectra of metal ($CdCl_2$) and ligand

Fig. 14 (c) show the interaction of $C_{15}H_{10}N_3ClO$ $CdCl_2$ comlpex with DNA, this show with increasing concentration of DNA in the drug solution the intensity of absorption band increase and λ_{max} also affected, so the consequence of DNA addition hyperchromism and slight blue shift appear.

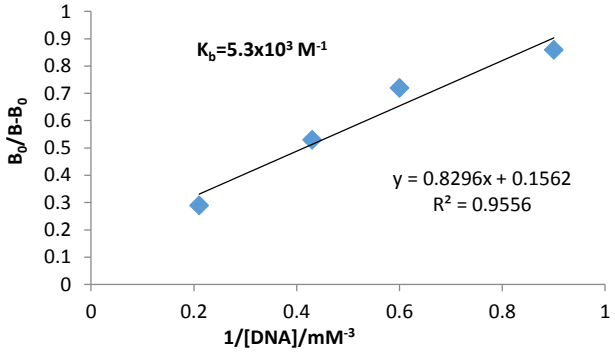

Fig. 15 Graph between $A_0/A\text{-}A_0$ *vs.* 1/ [DNA] plot

Fig. 15 represent the plot between $B_0/B\text{-}B_0$ *vs.* 1/[DNA], with the help of this plot we can determine the binding constant of Drug-DNA complex i.e. K_b= 5.3x10³ M⁻¹.

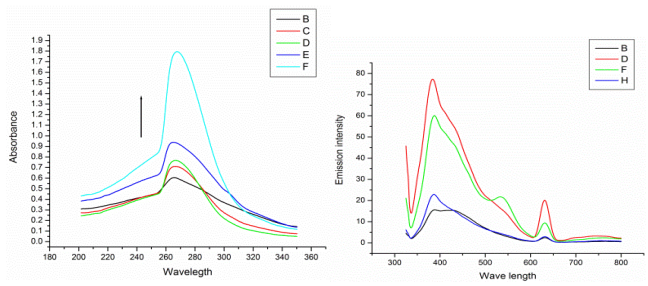

Fig. 16 (e) UV visible absorption spectra of $C_{15}H_{11}N_3O$ Cd Cl_2-DNA complex and arrow represent the increasing concentration of DNA in the solution. (f) Emission spectra of metal ($CdCl_2$) and ligand

Fig. 16(e) show the interaction of $C_{15}H_{10}N_3ClO$ $CdCl_2$ complex with DNA, this show with increasing concentration of DNA in the drug solution the intensity of absorption band increase and λ_{max} also affected, so the consequence of DNA addition hyperchromism and slight Bathochromic shift appear. Fig. 17 represent the plot between $C_0/C\text{-}C_0$ *vs.* 1/ [DNA], with the help of this plot we can find out the binding constant of Drug-DNA complex ie., K_b = 6.3x10³ M⁻¹.

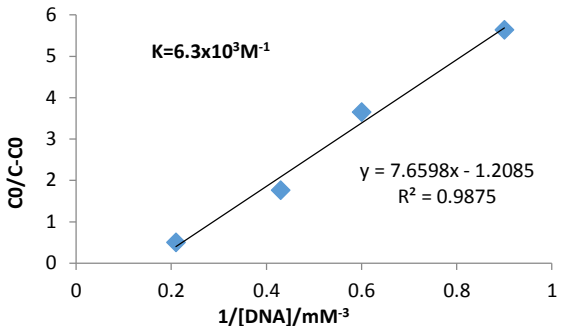

Fig. 17 Graph between C0/C-C0 *vs.* 1/ [DNA] plot

4. Conclusion

Electrochemical studies revealed that isatin-3-hydrazone and its derivatives are electro active as it undergoes oxidation and reduction processes at a carbon paste electrode. Compound 2a show two discrete one electron reductions, compound 2b show single two electron reduction peak and compound 2c show single two electron reduction peak so it reflect that in compound 2b and 2c second electron and proton transfer is very fast due presence of π aromatic ring system on –N=C carbon atom. Each compound show this reduction at different potential due to its substitution on carbon atom (-N=CR_1R_2), diffusion coefficient $D_0^{1/2}$ for compound 2a, 2b, 2c are 1.2x10⁻⁷, 2.0x10⁻⁷, 2.1x10⁻⁷ cm^2s^{-1} respectively. And after reduction a secondary amine is obtained and after that metal complex –DNA dealing/interaction has been investigated by UV-Visible spectroscopy. All spectral data and figures indicate that interaction between DNA and metal complexes (that is work as drug) takes place. In the solution metal complex 2a, 2b, 2c bind to DNA with binding constant k_b are 3.8x10³, 5.3x10³, 6.3x10³ M⁻¹ respectively. All complexes have protonated nitrogen so it is work as typical intercalators and must show hypochromism but in the presence of metal cation (Cd^{+2}) all complexes show hyperchromism with DNA.

Acknowledgement

The authors gratefully acknowledge UGC for financial assistance and Dr. H.S. Singh Gour University, Sagar (MP) for providing laboratory.

References

[1] P. Rani, V.K. Srivastava, A. Kumar, Synthesis and antiinflammatory activity of heterocyclic indole derivatives, Eur. J. Med. Chem. 39 (2004) 449-452.
[2] F. Palluotto, F. Campagna, A. Carotti, M. Ferappi, A. Rosato, C. Vitali, Synthesis and antibacterial activity of pyridazino[4,3-b]indole-4-carboxylic acids carrying different substituents at N-2, II Farmaco 57 (2002) 63-69.
[3] R.N. Goyal, A. Sangal, Studies of the behavior of 5-hydroxyindole-3- acetamide at a solid electrode, J. Electroanal. Chem. 578 (2005) 185-192.
[4] N. Hamaue, M. Minami, M. Hirafuji, M. Terado, M. Machida, N. Yamazaki, et al., Isatin based Schiff bases as Inhibitors of α-glucosidase: Synthesis, Characterization, In Vitro Evaluation and Molecular Docking Studies, CNS Drug Rev. 5 (1999) 331-346.
[5] A.E. Medvedev, A. Clow, M Sandler, V. Glover, Isatin: a link between natriuretic peptides and monoamines? , Biochem. Pharm. 52 (1996) 385-391.
[6] V. Glover, S.K. Bhattacharya, A. Chakrabarti, M. Sandler, The psychopharmacology of isatin: a brief review, Stress Med. 14 (1998) 225-229.
[7] V. Glover, M.A. Revely, M. Sandler, Human platelet monoamine oxidase activity in health and disease: a review. Biochem. Pharmacol. 29 (1980) 467-469.
[8] A.E. Medvedev, A. Clow, M. Sandler, V. Glover, Isatin: a link between natriuretic peptides and monoamines? Biochem. Pharmacol. 52 (1996) 385-391.
[9] A.E. Medvedev, O.Bussygyna, N. Pyatakova, N. Glover, I. Severina, Antipyretic action of isatin and its analogues in mice and rats , Biochem. Pharmacol. 63 (2002) 763-766.
[10] A.E. Medvedev, A. Clow, M. Sandler, V. Glover, Isatin: a link between natriuretic peptides and monoamines? Biochem. Pharmacol. 52 (1996) 385-391.
[11] E.L. Masden, J.M. Bollang, Anaerobic cometabolic conversion of benzothiophene by a sulfate-reducing enrichment culture and in a tar-oil-contaminated aquifer, Arch. Microbiol. 151 (1989) 71-77.
[12] A. Medvedev, J. Halket, V. Glover, Tribulin and endogenous MAO-inhibitory regulation in vivo, Med. Sci. Res. 22 (1994) 707-713.

[13] V.A. Mamedov, A.A. Kalinin, V.V. Yanilkin, Synthesis, structure, and electrochemical properties of 12,42 -dioxo- 21,31-diphenyl-7,10,13-trioxa-1,4(3,1)-diquinoxalina-2(2,3),3(3,2)-diindolizinacyclopentadecaphane, Rus. Chem. Bull. 56(10) (2007) 2060–2073.
[14] H. Xu, D. Wang, W. Zhang, W. Zhu, K. Yamamoto, L. Jin, Determination of isatin and monoamine neurotransmitters in rat brain with liquid chromatography using palladium hexacyanoferrate modified electrode, Anal. Chim. Acta 577 (2006) 207-210.
[15] M.Y. Wang, X.Y. Xu, J. Gao, A comparative study of electrochemical reduction of isatin and its synthesized Schiff bases at HMDE, J. Appl. Electrochem. 37 (2007) 705-709.
[16] J. Barek, J.C. Moreira, J. Zima, Electrochemical determination of trace Sudan I contamination in chili powder at carbon nanotube modified electrodes, Sensors 5 (2005) 148-151.
[17] B. Contabrana, A. Baamonde, F. Andres-Irellas, A. Hidalgo, A comparative study of electrochemical reduction of isatin and its synthesized Schiff bases at HMDE, Gen. Pharm. 2 (1990) 189-193.
[18] W. Zhang, Y. Zhao, H. Qigang, Synthesis and characterization of divalent metal complexes of the macrocyclic ligand derived from isatin and 1,2-diaminobenzene, Shengzhi Biyun. 9 (1989) 16-20.
[19] S.N. Pandeya, D. Sriram, G. Nath, Synthesis, antibacterial, antifungal and anti-HIV activities of Schiff and Mannich bases derived from isatin derivatives and N-[4-(4'-chlorophenyl)thiazol-2-yl] thiosemicarbazide, Eur. J. Pharm. Sci. 9 (1999) 25-30.
[20] G. Cerchiaro, A.M. Ferreira, Oxindoles and copper complexes with oxindole-derivatives as potential pharmacological agents, J. Braz. Chem. Soc. 17(2006) 1473-1480.
[21] A.E. Medvedev, V. Glover, Criteria for the evaluation of the functional importance of endogenous analogues of pharmacological regulators, Biochem. 3 (2007) 192-199.
[22] A.M. Oliveira Brett, V.C. Diculescu, J.A.P. Piedade, Electrochemical behaviour of 2,8-dihydroxyadenine at a glassy carbon electrode, Bioelectrochem. 55 (2002) 61-70.
[23] A.M. Oliveira Brett, J.A.P. Piedade, L.A. da Silva, V.C. Diculescu, Electrochemical DNA Sensors for Detection of DNA Damage, Anal. Biochem. 332 (2004) 321-332.
[24] A.M. Oliveira Brett, F.M. Matysik, Boron doped diamond electrode pre-treatments effect on the electrochemical oxidation of dsDNA, DNA bases, nucleotides, homopolynucleotides and biomarker 8-oxoguanine, Bioelectrochem. Bioener. 42 (1997) 111-120.
[25] R.N. Goyal, N. Kumar, N.K. Singhal, Electro-oxidation of atenolol at a glassy carbon electrode, Bioelectrochem. Bioener. 45 (1998) 47-55.
[26] O. Kennard, DNA–drug interactions, Pure Appl. Chem. 65(6) (1993) 1213–1222.
[27] R. Hajian, N. Shams, M. Mohagheghian, Study on the interaction between doxorubicin and deoxyribonucleic acid with the use of methylene blue as a probe, J. Braz. Chem. Soc. 20 (8) (2009) 1399–1405.
[28] R.S. Nicholson, I. Shain, Theory of Stationary Electrode Polarography. Single scan and cyclic methods applied to reversible, irreversible, and kinetic systems, Anal. Chem. 36 (1964) 706-712.
[29] H. Sun, J. Xiang, Y. Liu, L. Li, Q. Li, G. Xu, Y. Tang, A stabilizing and denaturing dual-effect for natural polyamines interacting with G-quadruplexes depending on concentration, Biochimie 93 (2011) 1351–1356.
[30] J. Jaumot, R. Gargallo, Experimental methods for studying the interactions between G-quadruplex structures and ligands, Curr. Pharmaceut. Des. 18(14) (2012) 1900–1916.
[31] C. Wei, J. Wang, M. Zhang, Spectroscopic study on the binding of porphyrins to (G4T4G4)4 parallel G-quadruplex, Biophys. Chem. 148 (2010) 51–55.
[32] K. Bhadra, G.S. Kumar, Interaction of berberine, palmatine, coralyne, and sanguinarine to quadruplex DNA: a comparative spectroscopic and calorimetric study, Biochim. Biophys. Acta 1810 (2011) 485–496.
[33] J. Liu, T. Zhang, T. Lu, L. Qu, H. Zhou, Q. Zhang, L. Ji, DNA-binding and cleavage studies of macrocyclic copper(II) complexes, J. Inorg. Biochem. 91 (2002) 269–276.
[34] M. Sirajuddin, S. Ali, A. Haider, N.A. Shah, A. Shah, M.R. Khan, Synthesis, characterization, biological screenings and interaction with calf thymus DNA as well as electrochemical studies of adducts formed by azomethine [2-((3,5-dimethylphenylimino)methyl)phenol] and organotin(IV) chlorides, Polyhedron 40(1) (2012) 19–31.
[35] M. Sirajuddin, S. Ali, N.A. Shah, M.R. Khan, M.N. Tahir, Synthesis, characterization, biological screenings and interaction with calf thymus DNA of a novel azomethine 3-((3,5 dimethylphenylimino)methyl)benzene-1,2-diol, Spectrochim. Acta A 94 (2012) 134–142.
[36] F. Arjmand, A. Jamsheera, DNA binding studies of new valine derived chiral complexes of tin(IV) and zirconium(IV), Spectrochim. Acta A 78 (2011) 45–51.
[37] H.A. Benesi, J.H. Hildebrand, Spectrophotometric investigation of the interaction of iodine with aromatic hydrocarbons, J. Am. Chem. Soc. 71 (1949) 2703–2707.

Cite this Article as: R. Das, A. Saxena, S. Saxena, G. Khan, Electrochemical study of some Schiff base by cyclic voltammetry and its metal complex - DNA interaction study by UV-visible spectroscopy, J. Adv. Electrochem. 1(1) (2015) 19-24.